

Pneumatic Artificial Muscles Force Modelling and the Position and Stiffness Control on the Knee Joint of the Musculoskeletal Leg

Jingtao Lei^{1*}, Jianmin Zhu²

¹School of Mechatronic Engineering and Automation
Shanghai University, Shanghai, China
E-mail: jtlei2000@163.com

²College of Mechanical Engineering
University of Shanghai for Science and Technology, Shanghai, China
E-mail: jmzhu6688@163.com

*Corresponding author

Received: March 21, 2016

Accepted: February 16, 2017

Published: March 31, 2017

Abstract: Pneumatic artificial muscles (PAMs) have properties similar to biological muscle and are widely used in robotics as actuators. A musculoskeletal leg mechanism driven by PAMs is presented in this paper. The joint stiffness of the musculoskeletal bionic leg for jumping movement needs to be analysed. The synchronous control on the position and stiffness of the joint is important to improve the flexibility of leg. The accurate force model of PAM is the foundation to achieving better control and dynamic jumping performance. The experimental platform of PAM is conducted, and the static equal pressure experiments are performed to obtain the PAM force model. According to the testing data, parameter identification method is adopted to determine the force model of PAM. A simulation on the position and stiffness control of the knee joint is performed, and the simulation results show the effectiveness of the presented method.

Keywords: Pneumatic artificial muscle, PAM force modelling, Bionic joint, Position and stiffness, Control algorithm.

Introduction

The bionic robot is one of the important researching directions. Quadruped robots have several advantages; they have better load performance, environment adaptability, less power consumption, have simpler structure as compared to six-legged or eight-legged robots, which have become a hot topic in the field of bionic robots [3, 6].

For a quadruped robot, the jumping movement has some advantages in the mobility and environmental suitability. The jumping movement is characterized by large instantaneous forces and short duration. Some jumping leg mechanisms have been developed worldwide. For a rigid robotics leg mechanism, it is difficult to meet the need of high-speed locomotion; otherwise, the musculoskeletal system is suitable for a jumping movement. PAMs allow dynamic and agile movements for the robot with the property of light weight and a large amount of energy converted in a short period of motion.

As PAMs have many desirable characteristics, such as flexibility similar to that of biological muscles, high power-to-weight ratio, high power-to-volume ratio, and inherent compliance, they have been widely used in various robotic systems [2]. The accurate output force model of PAM is the basis of motion control. It is difficult for the robotics system driven by PAMs to

obtain high-precision control effect. One of the reasons is that it is difficult to obtain accurate output power models. Although PAM has a simple structure, the factors that affect the output force are very complex, involving nonlinear compression, nonlinear deformation of the rubber, the effect of temperature on the gas and material, etc. These factors make it difficult to obtain an accurate mathematical model of PAM.

In recent years, researchers have attempted a variety of methods to determine a mathematical model of PAM, and these can be divided into two categories: theoretical modelling and experimental data modelling. Chou and Harnaford [1] used the equivalent power principle for PAM modelling. Tondu and Lopez [12] used the principle of virtual work for PAM modelling. As many factors were ignored, the model exhibits large errors with actual results. Tsagarakis and Caldwell [13] considered the non-cylindrical end of PAM in an inflated state, the rubber thickness, the friction and the elastic force of the rubber, and determined the PAM model in contraction and stretching states. Although the model has relatively higher accuracy, it is very complex, and hence difficult to use in an actual application.

In the experimental data modelling method, the mathematical model of PAM with some unknown parameters is first assumed. Second, experiments are performed to measure input/output PAM data. Third, the unknown parameters are determined by fitting the experimentally measured data, and the mathematical model of PAM is thus determined. Repperger et al. [10] used the experimental method, where PAM was regarded as a variable stiffness spring from the point of elasticity. When PAM is in the inflated state, it is regarded as hard spring stiffness. When PAM is in the elongation and deflated state, it is regarded as soft stiffness. The generated force of PAM includes steady state and transient spring force. In case of equal tension, the elastic parameters modulus and Poisson's ratio are used to express the characteristic parameters of PAM. Reynolds et al. [11] proposed that PAM is equivalent to a kind of a parallel model, composed of a spring, a buffer and a shrinking unit. The model is related to the PAM's internal pressure.

As highlighted above, an adequate PAM model cannot be obtained using purely theoretical analysis considering the characteristics of PAM.

When a quadruped robot moves with high-speed, there is a momentary contact force between the robot foot and the environment. A suitable control method is needed to achieve the robot's interaction with the environment in a flexible manner. This requires controlling both the joint trajectory and the joint stiffness so as to allow changes in real-time dynamic contract stiffness and load, and lead to good motion performance with high speed.

Nakamura et al. [7] have designed an antagonistic bionic joint driven by PAMs. They have adopted mechanical equilibrium model-based PI control method and have carried out an experimental study on the position and stiffness decoupling control. They have controlled the stiffness with a fixed value, and the joint position control accuracy is relatively low. Wang et al. [5, 14] have developed a quadruped robot driven by PAMs. They have adopted a basic position control method and model-based position control method to control the joint position. Their experimental investigations show the variation of joint stiffness with time. Xie et al. [15] have presented a lower limb mechanism driven by PAMs. Based on analyzing the output force model of PAM, a PID control algorithm is adopted.

In this paper, the experimental method is adopted to obtain a PAM model closer to the real system. A static equal pressure experiment is conducted to test the mechanical properties of

PAM. The experimental data are used to identify the axial force model. Based on the accurate force model of PAM, the PID and the BP (Back-propagation) control method on the position and stiffness of the knee joint are adopted for comparison. The simulation results are used to evaluate the effectiveness of the presented control method.

Musculoskeletal leg

The musculoskeletal leg is presented as shown in Fig. 1. The leg mechanism has three rotational joints, which are the side-swing hip joint, the forward/backward-swing hip joint and the knee joint.

The flexion/extension of the hip joint and the knee joint are all driven by two PAMs to increase their rotating range. PAM characteristics – tending to contract, and hard to elongate – are considered to arrange the PAMs of the knee joint. So the mechanical stretch structure is designed at the upper end of the PAM, which can compensate the lack of PAM elongation. The rotating range of the side-swing hip joint is 23° , the forward-swing hip joint is 10° and the knee joint is 55° , respectively [4].

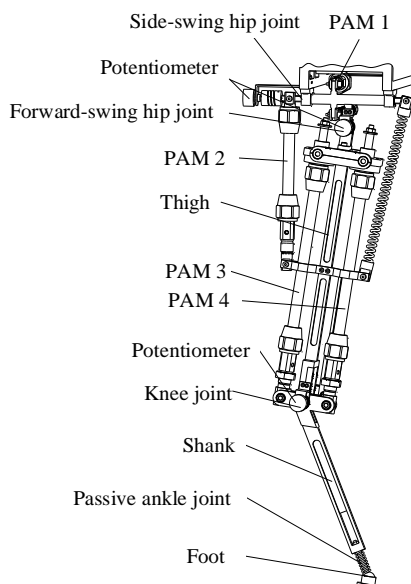


Fig. 1 Musculoskeletal leg mechanism

PAM modelling

For the theoretical model of PAM, the Chou model is widely used based on the equivalent power principle and the virtual work principle. The relationship between the PAM force, the inner pressure and the contraction ratio is as follows [9, 16]:

$$F(\varepsilon, p) = p \left(\frac{\pi d_0^2}{4} \right) (\beta_1 (1 - \varepsilon)^2 - \beta_2), \quad (1)$$

where p is the PAM inner pressure, β_1 and β_2 are constants related to the PAM parameters, $\beta_1 = 3 / \tan^2 \alpha_0$, $\beta_2 = 1 / \sin^2 \alpha_0$, α_0 is the initial braid angle, which is defined as the angle between the PAM axis and each thread of the braided sheath before expansion, ε is the contraction ratio expressed as $\varepsilon = (l_0 - l) / l_0$, l_0 is the initial length and d_0 is the initial diameter of the PAM.

Although the force model above describes the relationship between the axial output force, the inner gas pressure and the shrinkage rate of PAM, there is obviously a difference between this model and the experimental data because it ignores the rubber elastic, the wall thickness, the interaction between the rubber and the fiber bundle, and the deformation of the PAM end. Meanwhile, the relatively complex mathematical expression is not suitable for practical applications. In this paper, the experimental method is adopted to determine the PAM model. First, the mathematical model is assumed, and the parameters are determined by the experimental data and the parameters identification methods.

Hypothetical model of PAM

From viewpoint of practical control and application, the PAM model needs to be determined with reasonable balance between model complexity and parameter identification accuracy. On the one hand, the control precision of the system relies on the mathematical model of PAM. Therefore, the accuracy of the parameter identification directly affects the quality of control of the system. However, higher precision of the parameter identification will inevitably lead to a too long and complicated mathematical model, and this will have an impact on the real-time control system performance.

A mathematical model of PAM output force can be determined by the experimental method, which could show the relationship among the output force F , the gas pressure p and the contraction rate ε . Considering the nonlinear relation between the output force and the displacement of PAM, an improved Tondu-Lopez model [8] is proposed as:

$$F = (a_1 + a_2 \cdot p) + (b_1 + b_2 \cdot p) \cdot \varepsilon + (c_1 + c_2 \cdot p) \cdot e^{-\mu\varepsilon}, \quad (2)$$

where $a_1, a_2, b_1, b_2, c_1, c_2$ are the parameters which can be determined using the least-squares method, μ is the nonlinear attenuation coefficient describing the shrinkage rate ε of PAM.

Experimental system

The experimental system is composed of PAMs, a stretching device (including reducer, with a reduction ratio of 10), a force sensor, a pressure sensor, a proportional valve, a data acquisition card and a computer. The stretching device is composed of a step motor, a lead screw with 5 mm pitch and guide rails, as shown in Fig. 2. The PAM type used is MAS-10-180N-AA-MC-O from FESTO Company. The range of working pressure of PAM is 0-0.8 MPa, and the maximum output force is 630 N. The maximum contraction rate is 25%, and the maximum initial tension rate is 3%. The left PAM is fixed to the stretching platform and the right PAM is fixed to the step motor with a force sensor. The pressure gas from the air compressor is charged into the PAM through the filter regulator and the proportional valve.

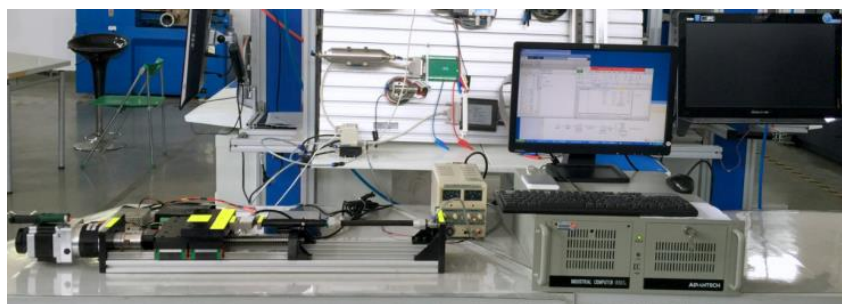


Fig. 2 Experimental system for determining the PAM model

The hardware used in the experimental system is described in Table 1.

Table 1. Hardware used in the experiment

Item	Model	Company
PAM	MAS-10-180N-AA-MC-O	FESTO
Force sensor	TSH-200	METTLER TOLEDO
Pressor sensor	SDE1-D10-G2-W18-L-PU-M8	FESTO
Proportional valve	ITV0050-3ML	SMC
Computer	IPC-610L	ADVANTECH
Data acquisition card	PCI-6281	NI
Junction box	SCB-68A	NI

Parameters identification

For the MAS-10-180N-O-MC-O type of PAM, the initial length and the initial diameters were 180 mm and 10 mm, respectively. Generally, different experimental methods with equal length, equal pressure or equal force are adopted to obtain the PAM model. In this paper, the equal pressure experimental method is adopted to identify the parameters of the PAM model.

The equal pressure experiment is performed to obtain the PAM characteristic curve under the pressures from 0 to 6 bar with 13 different values. The proportional valve is used to ensure the pressure stability. The motor driver is used to control the step motor and drive a screw to achieve the stretch or contraction of PAM. During the experiment, the pulse number of the motor was set so as to control the stretch/contraction rate at 0.2 mm/s, which implies that the PAM stretch/contract length will reach 1 mm every 5 s. 1000 data points are collected within 1 s after each 5 s delay for obtaining stable data of PAM pressure and output force.

The experimental process includes adjusting the experimental device, determining the boundary values, unloading test, load testing and saving the collected data.

In order to obtain sufficient data for parameters identification and PAM modelling, the stretch and contract experiment was repeated five times at each constant pressure. 13 characteristic curves of the 5-groups data were obtained, as shown in Fig. 3. The curves show that the equal pressure characteristic curve of PAM has directivity, i.e., PAM exhibits similar mechanical properties during the process of loading and unloading, and the relationship between the output force and the shrinkage rate is nonlinear.

According to the rate of change of force attenuation, the contraction rate of PAM MAS-10-180N-AA-MC-O was determined as $\mu = 0.3$. Thus, the PAM model was determined as:

$$F = (-245.8 + 109 \cdot p) + (3.216 - 3.442 \cdot p) \cdot \varepsilon + (255.6 - 13.18 \cdot p) \cdot e^{-0.3\varepsilon}. \quad (3)$$

Model validation

The experimental mathematical model of PAM MAS-10-180N-AA-MC-O is based on the static isobaric pressure experiments and the parameters identification method. Whether the experimental model of PAM is correct has to be verified. Changing the gas pressure, the loading and unloading PAM experiments are performed. The gas pressure is set to 2 bar, 3 bar, 4.5 bar and 6 bar, respectively. The loading and unloading isobaric experiments are performed. The PAM axial force is calculated by the experimental model and compared with the experimental data to verify the correctness of the muscle model. At the same time, the PAM force of the experimental model is compared with the force by the theoretical model. As shown in Fig. 4, the loaded experimental data is in blue color, and the unloading

experimental data is the red curve. The purple curve is the PAM force calculated by the experimental model presented in this paper, and the green curve is the PAM force calculated by the Chou model.

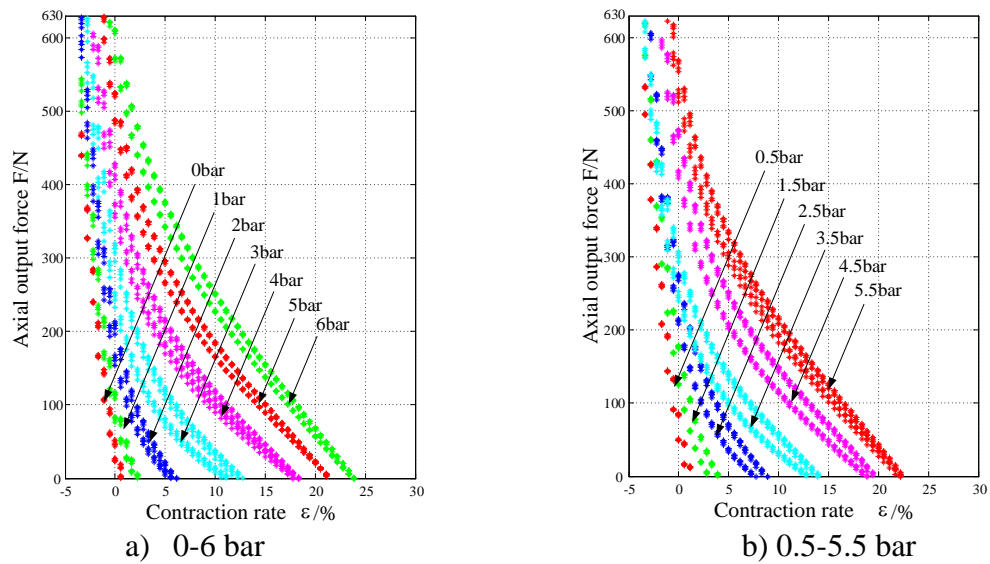


Fig. 3 Isobaric feature test curves

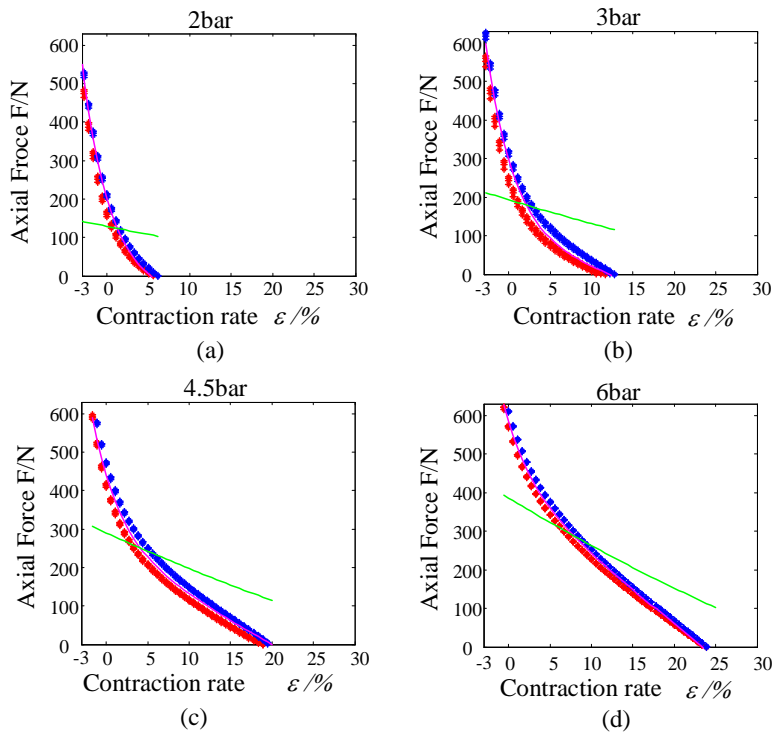


Fig. 4 Force comparison between the experimental data (blue and red),
the experimental model (purple) and the theoretical model (green)

As can be seen in Fig. 4, the experimental model curve (purple) is very close to the loading data (blue) and the unloading (red) data. But the experimental model curve (purple) is quite different with the theoretical model curve (green). It is shown that the mathematical model of PAM by the experimental method can reflect the actual characteristics of PAM, and verify the correctness of the experimental modeling method.

Joint position and stiffness control simulation

Control method

Joints play very important role in the robot locomotion. In order to achieve high-speed locomotion of quadruped robot, it is necessary to control the position and stiffness of the joint. The forward-swing hip joint and the knee joint play a key role in jumping movement. In this paper, the position and stiffness synchronization control on the knee joint is performed by simulations. The conventional PID and BP neural network control methods are adopted. The simulation is performed to verify the effectiveness and control accuracy of the joint position and stiffness synchronization control method. In order to contrast the control precision, the same PID controller parameters are used in two methods.

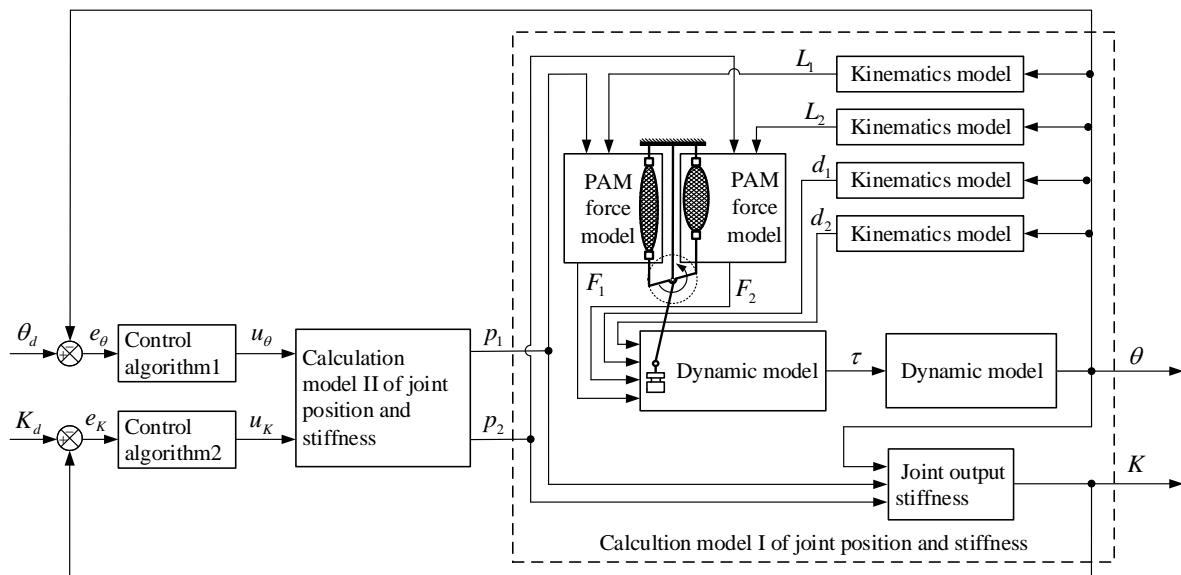


Fig. 5 System schematics of joint stiffness and position synchronization control

Kinematics and dynamics

The knee joint model is shown in Fig. 6: τ is the joint driving torque; m_1 and m_2 are the equivalent mass of the knee joint and the external load, respectively; l_1 and l_2 are the distances from the point of the joint rotating center to the center point C_1 of the knee equivalent mass and to the point C_2 , respectively; F_1 and F_2 are the axial output forces of PAMs, and d_1 and d_2 are the arm lengths of the corresponding forces.

According to geometry relationship, the kinematics model of knee joint can be obtained as:

$$L_1 = \sqrt{(H + r \sin \theta)^2 + (r - r \cos \theta)^2} - (L_u + L_d) \quad (4)$$

$$L_2 = \sqrt{(H - r \sin \theta)^2 + (r - r \cos \theta)^2} - (L_u + L_d)$$

$$d_1 = \frac{r(H \cos \theta + r \sin \theta)}{\sqrt{(H + r \sin \theta)^2 + (r - r \cos \theta)^2}} \quad (5)$$

$$d_2 = \frac{r(H \cos \theta - r \sin \theta)}{\sqrt{(H - r \sin \theta)^2 + (r - r \cos \theta)^2}}$$

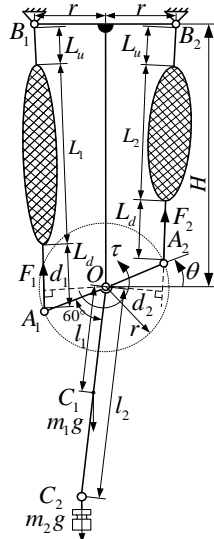


Fig. 6 Knee joint mechanism model

The expected driving torque of the knee joint can be derived as:

$$\tau_e = (J + m_1 l_1^2 + m_2 l_2^2) \ddot{\theta} + c \dot{\theta} + (m_1 l_1 + m_2 l_2) g \sin(\pi/6 - \theta), \quad (6)$$

where J is the equivalent moment of inertia of the leg mechanism and c is the joint damping coefficient.

The actual driving torque of the knee joint can be derived by the torque balance equation. The generalized forces acting on the knee joint mechanism are: PAM output forces F_1 and F_2 , joint driving torque τ , knee equivalent gravity $m_1 g$, external load equivalent gravity $m_2 g$.

Then, the joint driving torque of the knee joint is:

$$\tau = (m_1 l_1 + m_2 l_2) g \sin(\pi/6 - \theta) + F_2 d_2 - F_1 d_1, \quad (7)$$

where F_1 and F_2 can be calculated by Eq. (3).

The joint stiffness can be derived by taking a derivative of the driving torque with respect to the joint variable [14]:

$$K = \frac{d\tau}{d\theta} \quad (8)$$

where K is joint stiffness, τ is joint torque vector and θ is joint angular displacement.

Table 2 presents the values of the parameters.

Results and analysis

Taking the knee joint as an example, a synchronization control simulation of the joint position and stiffness is conducted. Setting the desired joint position as a sine function and the desired stiffness as the constant value or step value, the conventional PID and BP control algorithms are adopted and the simulations are performed to compare the control effectiveness. The joint position and stiffness simulation results are shown in Fig. 7 and Fig. 8.

Table 2. Parameters

Parameter, Unit	Value
PAM initial diameter D_0 , m	0.01
PAM initial braid angle α_0 , °	25
Initial length of rubber balloon L_0 , m	0.18
Length sum of connectors $L_u + L_d$, m	0.19
Equivalent joint length H , m	0.37
Equivalent joint radius r , m	0.03
Equivalent mass of knee joint m_1 , kg	0.5
External load equivalent mass m_2 , kg	0.5
Distance l_1 , m	0.1
Distance l_2 , m	0.2
Equivalent moment of inertia J , kg·m ²	0.02
Joint damping coefficient c , N·s/m	0.015

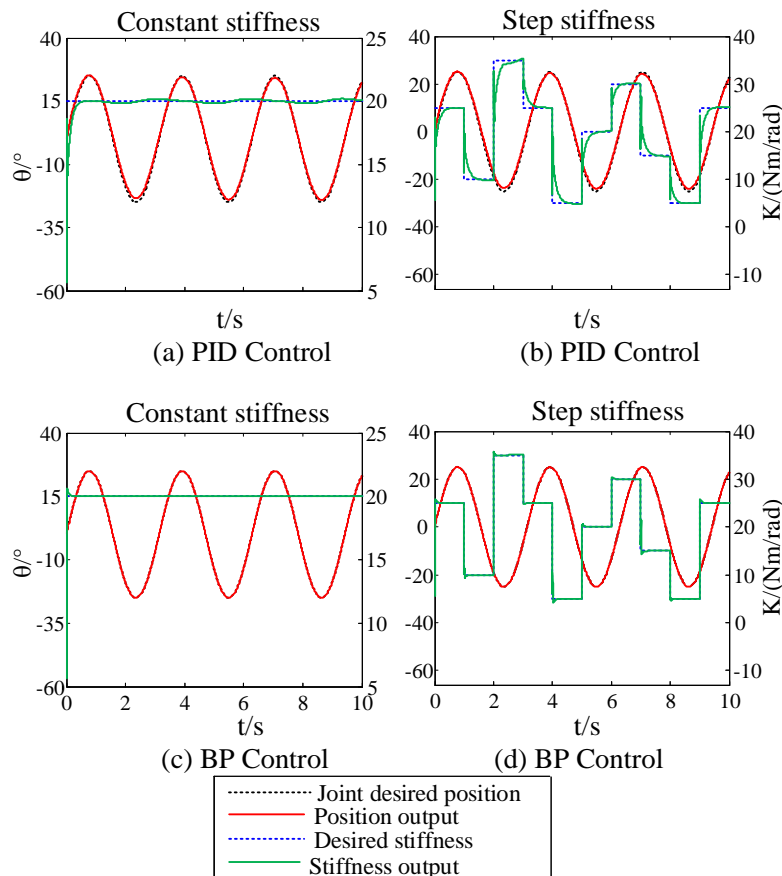


Fig. 7 Control results on the joint position and stiffness

Fig. 7 shows the simulation results of the joint position and stiffness by using the conventional PID and BP control methods and under different desired joint stiffness, which are constant value or step stiffness. Fig. 7(a) presents the simulation results concerning the constant stiffness and Fig. 7(b) presents the simulation results concerning the step stiffness, both obtained by the conventional PID control method. Fig. 7(c) presents the simulation results concerning the constant stiffness and Fig. 7(d) presents the simulation results concerning the step stiffness, both obtained by the BP control method.

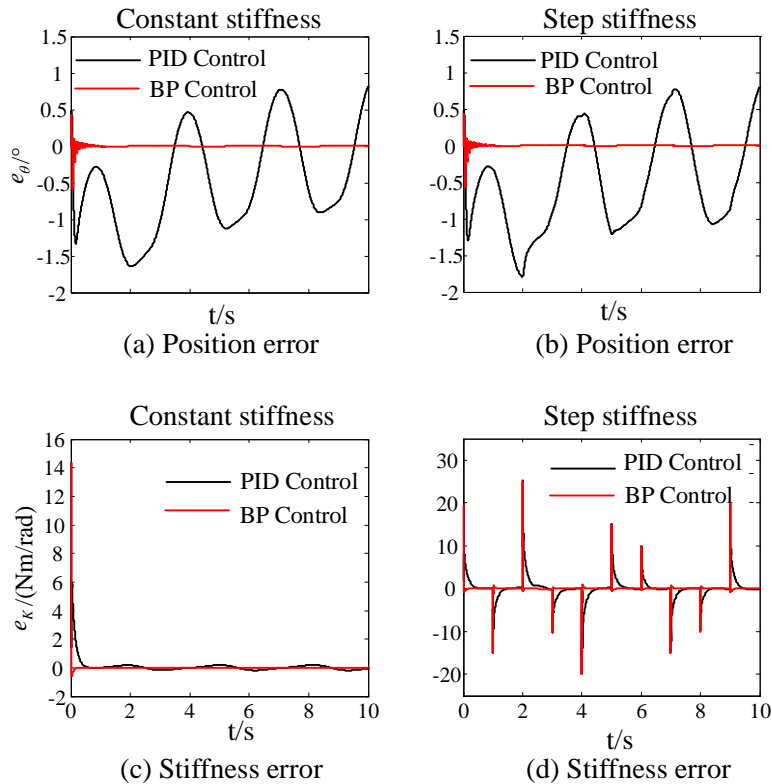


Fig. 8 Error curve of the joint position and stiffness

Fig. 8 shows the error curve of the joint position and stiffness by using the conventional PID and BP control methods under different desired joint stiffness. Fig. 8(a) shows that the desired joint stiffness is a constant value, and Fig. 8(b) shows that the desired joint stiffness is a step value. The PID and the BP control methods are adopted and the tracking errors of the joint position are compared. When the PID control method is adopted, under two kinds of the desired stiffness, the tracking errors of the joint position are large. When the BP control method is adopted, the tracking errors of the joint position are all small under two kinds of the desired stiffness. The tracking errors of the joint stiffness are shown in Fig. 8(c) concerning the constant stiffness and in Fig. 8(d) concerning the step stiffness. Both the PID and the BP control methods are compared. The joint stiffness adjustment time by PID is relatively longer than that of the BP control method. The tracking errors of joint stiffness by the PID and the BP control methods are compared.

The simulation results show that the joint stiffness varying will cause joint position fluctuations, and the joint position changing will cause joint stiffness fluctuations. The joint position and stiffness are coupled with each other.

Conclusions

A musculoskeletal leg driven by PAMs is presented. The experimental method is presented to obtain an accurate force model of PAM closer to the real situation. Static equal pressure experiments are performed and the curve fitting method is adopted to identify the model parameters. The correctness of the PAM modeling method presented in this paper is verified by simulation. For the musculoskeletal leg, synchronous control on the position and stiffness of the knee joint is performed to improve the flexibility for high-speed movement. The PID and BP control algorithms are adopted for comparison. The simulation results show that the BP control algorithm could achieve better control accuracy.

Acknowledgments

This research is supported by National Natural Science Foundation of China Grant Number 51375289, National Natural Science Foundation of Shanghai Grant Number 13ZR1415500.

References

1. Chou C. P., B. Hannaford (1996). Measurement and Modeling of McKibben Pneumatic Artificial Muscle, IEEE Transaction on Robotics and Automation, 12(1), 90-102.
2. Georgios A., N. Georgios, M. Stamatis (2011). A Survey on Applications of Pneumatic Artificial Muscles, Proceedings of the 19th Mediterranean Conference on Control and Automation, Corfu, 1439-1446.
3. Kitano S., S. Hirose, G. Endo, E. F. Fukushima (2013). Development of Lightweight Sprawling-type Quadruped Robot TITAN-XIII and Its Dynamic Walking, Proceedings of the IEEE/RSJ International Conference on Intelligent Robots and Systems, Tokyo, 6025-6030.
4. Lei J. T., J. D. Wu (2016). Bionic Jumping Dynamics of the Musculoskeletal Leg Mechanism for Quadruped Robots, High Technology Letters, 22(3), 1-8.
5. Li M., X. Wang, W. Guo, P. Wang, L. Sun (2014). System Design of a Cheetah Robot toward Ultra-high Speed, International Journal of Advanced Robotic Systems, 11(10), 707-714.
6. Meng Y. C., S. Kim (2014). Enabling Force Sensing During Ground Locomotion: A Bio-inspired, Multi-axis, Composite Force Sensor Using Discrete Pressure Mapping, IEEE Sensors Journal, 14(5), 1693-1703.
7. Nakamura T., D. Tanaka, H. Maeda (2011). Joint Stiffness and Position Control of an Artificial Muscle Manipulator for Instantaneous Loads Using a Mechanical Equilibrium Model, Advanced Robotics, 25(3), 387-406.
8. Narioka K., A. Rosendo, A. Sproewitz, K. Hosoda (2012). Development of a Minimalistic Pneumatic Quadruped Robot for Fast Locomotion, Proceedings of the IEEE International Conference on Robotics and Biomimetics, Guangzhou, 307-311.
9. Pujana-Arrese A., A. Mendizabal, J. Arenas, R. Prestamero, J. Landaluze (2010). Modelling in Modelica and Position Control of a 1-DoF Set-up Powered by Pneumatic Muscles, Mechatronics, 20(5), 535-552.
10. Repperger D., K. Johnson, C. Phillips (1999). Nonlinear Feedback Controller Design of a Pneumatic Muscle Actuator System, Proceedings of the American Control Conference, San Diego, California, New York, 1525-1529.
11. Reynolds D., D. Repperger, C. Phillips, G. Bandry (2003). Modeling the Dynamic Characteristics of Pneumatic Muscle, Annals of Biomedical Engineering, 31(3), 310-317.
12. Tondu B., P. Lopez (2000). Modeling and Control of McKibben Artificial Muscle Robot Actuators, IEEE Control System Magazine, 20(2), 15-38.
13. Tsagarakis N., D. G. Caldwell (2000). Improved Modeling and Assessment of Pneumatic Muscle Actuators, Proceedings of the IEEE International Conference on Robotics & Automation, San Francisco, California, New York, 3641-3646.
14. Wang X., M. Li, W. Guo, P. Wang, L. Sun (2013). Development of an Antagonistic Bionic Joint Controller for a Musculoskeletal Quadruped, Proceedings of the IEEE/RSJ International Conference on Intelligent Robots and Systems, Tokyo, 4466-4471.
15. Xie H., K. Chen, Y. Yang, F. Li (2015). Artificial Leg Design and Control Research of a Biped Robot with Heterogeneous Legs Based on PID Control Algorithm, International Journal Bioautomation, 19(1), 95-106.
16. Yamada Y., S. Nishikawa, K. Shida, R. Niiyama, Y. Kuniyoshi (2011). Neural-body Coupling for Emergent Locomotion: A Musculoskeletal Quadruped Robot with Spinobulbar Model, Proceedings of the IEEE/RSJ International Conference on Intelligent Robots and Systems, San Francisco, California, 1499-1506.

Assoc. Prof. Jingtao Lei, Ph.D.E-mail: jtlei2000@163.com

Jingtao Lei received her Ph.D. degree from Beihang University, China in 2007. She was a postdoctoral fellow at Robotics Institute of Beihang University from 2007 to 2009. She is currently a visiting scholar at The University of Sheffield. She is an Associate Professor, working at School of Mechatronic Engineering and Automation, Shanghai University, China. She is a Member of the CLAWAR Association. Her main research interests include bionic robots and modular technology on service robots.

Prof. Jianmin Zhu, Ph.D.E-mail: jmzhu6688@163.com

Jianmin Zhu received his Bachelor degree in 1991 and his Master degree in 1994, both from Luoyang Institute of Technology, and have a Ph.D. in 2000 from the Huazhong University of Science and Technology. Now he is a Professor and a Ph.D. supervisor in the University of Shanghai for Science and Technology. His main research interests are precision measurement technology, intelligent control of mechatronic systems.



© 2017 by the authors. Licensee Institute of Biophysics and Biomedical Engineering, Bulgarian Academy of Sciences. This article is an open access article distributed under the terms and conditions of the Creative Commons Attribution (CC BY) license (<http://creativecommons.org/licenses/by/4.0/>).